J. Appl. Phys. **103** 07C505 (2008)

Thickness dependence of magnetic film edge properties in $Ni_{80}Fe_{20}$ stripes

Robert D. McMichael*
Metallurgy Division, National Institute of Standards and Technology, 100 Bureau Drive, Gaithersburg, Maryland USA

C. A. Ross and Vivian P. Chuang
Department of Materials Science and Engineering, Massachusetts Institute of Technology, Cambridge, MA, USA.
(Dated: September 25, 2008)

Measurements of "trapped spinwave" edge modes in transversely magnetized stripe arrays of $Ni_{80}Fe_{20}$ largely confirm previous theoretical predictions for the thickness dependence of the edge saturation field $H_{\rm sat}$ and the effective out-of-plane edge anisotropy field H_2. The stripes were patterned using optical interference lithography with film thicknesses in the range from 10 to 65 nm. Large linewidth values for edge modes relative to bulk modes indicate inhomogeneity of the edges. Elimination of an antireflective coating underlayer dramatically decreases the edge mode linewidth without affecting the bulk mode linewidth.

PACS numbers: 75.75.+a, 76.50.+g, 85.70.Ay

I. INTRODUCTION

Magnetic nanostructures form the foundation of several important technologies in data storage and they also underpin developments in spin transfer torque and patterned-media hard drives. Because the ratio of perimeter to area increases as these structures are scaled down, measurement of the magnetic properties of thin film edges will become increasingly important for magnetic nanodevice design and modeling.

Ferromagnetic resonance of the "trapped spinwave" edge modes[1, 2] has emerged as a precise method for measuring the magnetic properties of the thin film edges[3, 4]. In films that are magnetized perpendicular to a film edge, demagnetization fields reduce the local field near the edge, creating conditions for the localized precession of an edge mode. The relationship between the applied field and the resonance frequency of the edge mode yields two edge-sensitive parameters: $H_{\rm sat}$, which is the field required to saturate the magnetization perpendicular to the edge, and H_2 which is an effective out-of-plane shape anisotropy for the edge mode.

Several models have predicted the dependence of $H_{\rm sat}$ and H_2 on thickness for ideal edges. These models, described in detail in ref. 5, include micromagnetic models of the edge magnetization dynamics, a stability analysis of the magnetization near the edge and a macrospin model. The macrospin model approximates the edge mode dynamics with magnetization precession in an equivalent ellipsoidal cylinder having major and minor axes equal to the film thickness t and an effective edge width $d_{\rm e}$, and yields a simple approximate expression for $H_{\rm sat}$;

$$H_{\rm sat} = \frac{M_s}{2}\frac{t}{t+d_{\rm e}}, \tag{1}$$

where $M_{\rm s}$ is the saturation magnetization. Fitting to the micromagnetic model results yields $d_{\rm e} = 4.6\, l_{\rm ex} \approx 26$ nm for $Ni_{80}Fe_{20}$. Further, the macrospin model predicts a relationship between $H_{\rm sat}$ and H_2 that is confirmed by the micromagnetic models.

$$H_2 = M_{\rm s} - 3H_{\rm sat}. \tag{2}$$

This paper describes measurements of the thickness dependence of the edge parameters, measurements of the sensitivity of the edge parameters to patterning methods, and analysis of edge parameter variations through edge mode linewidths.

II. PROCEDURE

Our main series of samples were patterned by optical interference lithography on Si substrates. A trilayer resist stack was used, consisting of an antireflective coating (ARC), a thin, sputtered, silicon oxide layer, and finally a resist layer deposited sequentially on a silicon substrate[6]. The resist was exposed and developed to create a grating pattern in the resist. A $Ni_{80}Fe_{20}$ film was then evaporated onto the substrate using a electron-beam evaporation. The resist, along with its $Ni_{80}Fe_{20}$ overlayer, were lifted off using a resist stripper, soaking for 90 s at 50 C and sonicating for 30 s at 24 C. Film thicknesses range from 10 nm to 65 nm in stripes that are approximately 450 nm wide with a period of 800 nm. A micrograph of one of the samples is shown in Fig. 1.

Two special samples were prepared to test the sensitivity to patterning conditions. One special sample was prepared using the ARC as the mask. For this sample,

*Electronic address: rmcmichael@nist.gov

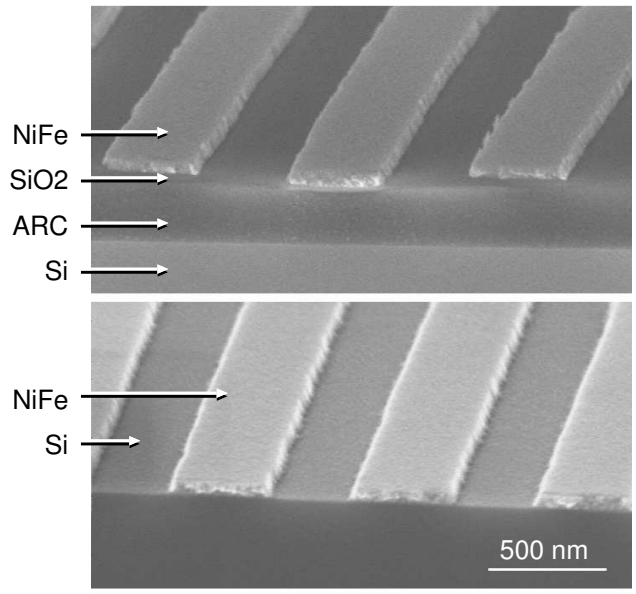

FIG. 1: Top: SEM micrograph of 40 nm thick stripes on an anti-reflective coating (ARC) and SiO_2 underlayer. Bottom: 40 nm thick stripes on Si created using the ARC and SiO_2 as a mask layer.

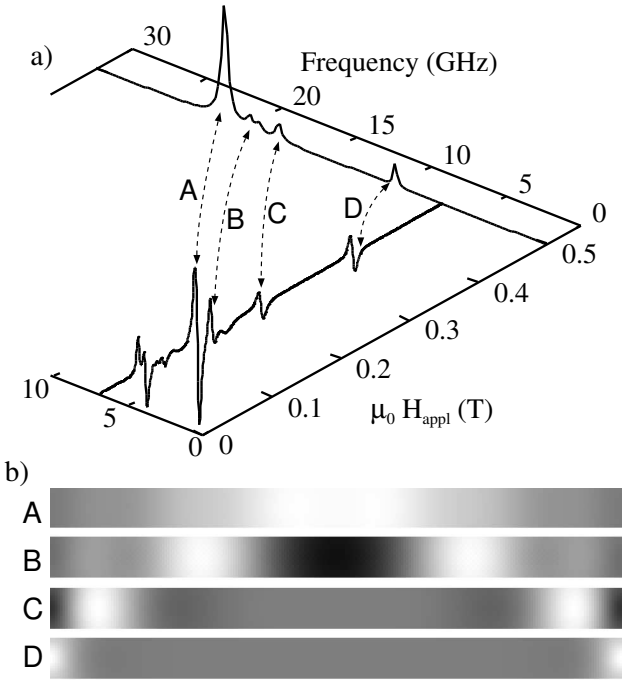

FIG. 2: a) The lower curve is a ferromagnetic resonance spectrum of the 40 nm thick stripes on Si measured at 7 GHz. The upper curve is an absorption curve for $H_{\rm appl} = 0.5$ T obtained by micromagnetic modeling that shows corresponding resonances. b) Mode profile images from the micromagnetic modeling. Identification of the modes is made by comparing mode intensities and mode sequences.

reactive ion etching was used to transfer the stripe pattern to the ARC layer, creating a mask of ARC material. A 40 nm film of $Ni_{80}Fe_{20}$ was then deposited on the exposed thermal oxide of the Si wafer, followed by liftoff of the ARC. This sample differs from the main sample series in that the mask layer is ARC rather than resist, and in that the $Ni_{80}Fe_{20}$ is deposited on the native oxide of the Si wafer rather than sputtered SiO_2 on top of ARC.

In another sample, we tested the sensitivity to resist liftoff conditions. A stripe array with thickness 65 nm was prepared using the resist mask and a reduced liftoff soak time of 60 s.

The edge modes were detected with the sample placed face down on a coplanar waveguide. Bulk mode and edge mode resonances were detected as decreases in transmitted microwave signal as a function of microwave frequency and applied field. Enhanced signal to noise was achieved by adding 80 Hz applied field modulation and using lockin detection of the transmitted signal[3, 4].

Alignment is important for measurements of the edge mode at low frequencies[3]. To align the stripes perpendicular to the field direction, the edge mode resonance field was recorded with 7 GHz excitation at 1° intervals in a 10° region near perpendicular. Fitting of this data allowed alignment of the field perpendicular to the stripe axis with a accuracy of 0.1°.

III. RESULTS

An example field-swept FMR spectrum is shown in Fig. 2a. The distinct resonances in this spectrum are identified by comparison with micromagnetic modeling[7] of the stripe's absorption spectrum. The calculation involves a sequence of ground state, field pulse, and ring down calculations followed by Fourier transform of the ring down response[8]. Fig. 2b shows modeled mode profiles of the labeled modes. Each rectangle corresponds to the cross section of a 450 nm × 40 nm stripe. Modes

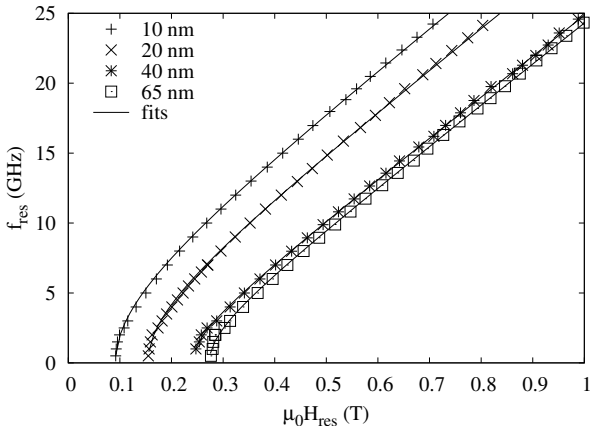

FIG. 3: Field dependence of edge mode resonance frequency for the stripe arrays deposited on anti-reflective coating. The solid lines are fits to Eq. (3).

A and B have large amplitudes but opposite phases at the center of the stripe as indicated by light and dark contrast. Modes C and D are localized near the edges of the stripe with very small amplitudes (grey contrast) in the central part of the stripe. Multiple edge modes have been previously observed for fields below $H_{\rm sat}$[9]. The rest of this paper will focus on the behavior of mode D, which we will refer to as the edge mode.

For each sample, edge mode resonances were recorded from 0.5 to 25 GHz. The magnetic film edge properties for each thickness were determined by fitting the field dependence of the edge mode frequency to

$$f(H) = \frac{\mu_0\gamma}{2\pi}\left[(H_{\rm appl} - H_{\rm sat})(H_{\rm appl} + H_2)\right]^{1/2}, \qquad (3)$$

using $H_{\rm sat}$ and H_2 as fitting parameters. Example fits are plotted in Fig. 3 The gyromagnetic ratio γ was held constant at 29 GHz/T, and the asymptotic standard errors of the fits were less than ± 1 mT for $H_{\rm sat}$, and less than ± 4 mT for H_2.

To approximate edge property values that are independent of stripe widths and array periods the fit values of $H_{\rm sat}$ and H_2 are corrected for interactions with the other stripes in the array and for the field at one edge of a stripe due to magnetostatic charges at the opposite edge. These two corrections largely cancel, and the net correction reaches a maximum value of 80 mT in the thickest stripes. Corrected values of $H_{\rm sat}$ and H_2 are plotted in Fig. 4 with the results of three models for the thickness dependence of $H_{\rm sat}$ in stripes with ideal edges. While the measured values follow the trend predicted by the models, the measured edge saturation fields are lower than the modeled values for ideal edges, consistent with previous measurements of edge saturation field[3, 4, 10, 11]. Many edge conditions, including tilting of the edge surface[4, 10], surface anisotropy and/or dilution of the magnetization near the edge may explain this difference[5].

The edge parameters are relatively insensitive to the liftoff conditions. Reducing the liftoff soak time of the 65 nm thick sample by 33% produced negligible changes. Also, changing the mask material from resist to ARC has a small effect on the edge parameters, although it does have a significant effect on the edge mode linewidth, as discussed below.

Linewidth values for edge modes are plotted as a function of frequency in Fig. 5. The peak in the linewidth at low frequencies is largely an artifact of overlapping resonances. While this paper largely focuses on the edge mode for fields greater than $H_{\rm sat}$ there is also a distinct edge resonance for fields below $H_{\rm sat}$ where the edge magnetization precesses around a canted ground state[1, 2, 9, 12]. As the frequency approaches zero, the two resonances of the canted-ground-state edge mode and the aligned-ground-state edge mode approach each other from opposite sides of $H_{\rm sat}$. See Fig. 1 of ref. 5. These overlapping resonances give the appearance of a single, broadened resonance at low frequencies. Since the low

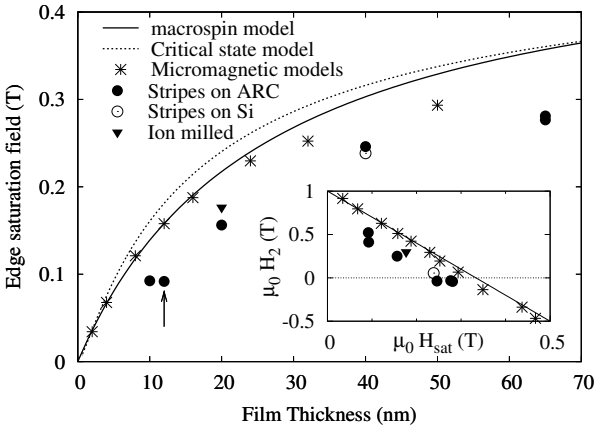

FIG. 4: Measured thickness dependence of the edge saturation field. Inset: relationship between $H_{\rm sat}$ and H_2. The "ion milled" point is described in ref. 4, and the point marked with the arrow is from ref. 3. Model results are reproduced from ref. 5.

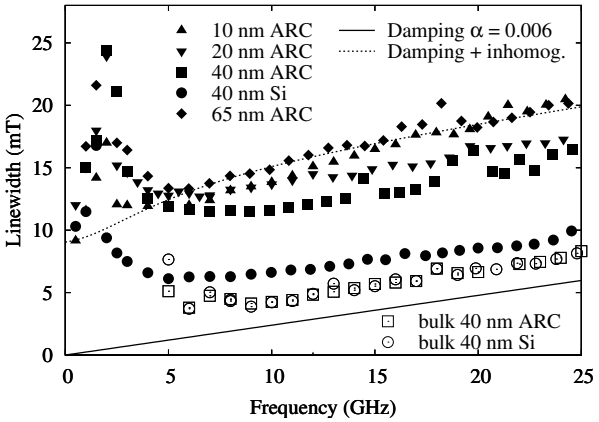

FIG. 5: Edge mode resonance linewidths (filled symbols) as a function of frequency. Edge mode linewidth is significantly lower for the stripes on Si. Bulk mode linewidths (open symbols) for the 40 nm thick films are shown for comparison. The solid line is the intrinsic linewidth predicted for a Gilbert damping parameter $\alpha = 0.006$.; the dotted line includes an inhomogeneous broadening expected for a 3.7 mT standard deviation of $H_{\rm sat}$.

frequency linewidth peaks can be explained as artifacts, we focus our attention on the higher frequencies.

The linewidths for the edge mode in the stripes on ARC are significantly larger than the linewidths for the bulk modes in these stripes. The FMR linewidth is often interpreted as the sum of an intrinsic component that is proportional to the damping parameter α, and an inhomogeneous contribution ΔH_0.

$$\Delta H = \frac{2\alpha}{\sqrt{3}}\frac{\omega}{\gamma} + \Delta H_0. \qquad (4)$$

To first approximation, the difference between the bulk linewidths and the edge linewidths is close to an addi-

tive constant, suggesting an inhomogeneous broadening mechanism rather than an increase in α at the edge, which would appear as an increase in slope.

The large difference between the bulk mode linewidths and the edge mode linewidths may be partly explained by variations in the edge parameters. A Gaussian distribution of $H_{\rm sat}$ values with standard deviation $\sigma_{\rm sat}$ will produce a contribution to the peak-to-peak linewidth,

$$\Delta H_0 = 2\sigma_{\rm sat}\frac{4H_{\rm appl} - 3H_{\rm sat} + H_2}{2H_{\rm appl} - H_{\rm sat} + H_2} \qquad (5)$$

Here we have assumed that variations in H_2 are correlated with variations in $H_{\rm sat}$ through Eq. (2). This contribution to the linewidth is plotted in Fig. 5. This inhomogeneous contribution to the linewidth is included in the dotted line in plotted in Fig. 5 for $\sigma_{\rm sat} = 3.7$ mT.

The line width of the edge modes for the stripes on Si patterned by an ARC mask are an interesting exception, having a linewidth that is nearly as low as the bulk modes. This result suggests that the stripes on Si have more homogeneous edges. However, comparison of SEM images of the stripes in Fig. 1 does not reveal any clear differences on length scales that are resolved by the microscope.

In conclusion, the measured thickness dependence of magnetic film edge parameters largely follows model predictions, although there are significant differences due to the non-ideal edge conditions.

The authors acknowledge the technical assistance of A. Band of the NIST Center for Nanoscale Science and Technology.

[1] J. Jorzick, S. O. Demokritov, B. Hillebrands, M. Bailleul, C. Fermon, K. Y. Guslienko, A. N. Slavin, D. V. Berkov, and N. L. Gorn, Phys. Rev. Lett. **88**, 047204 (2002).
[2] J. P. Park, P. Eames, D. M. Engebretson, J. Berezovsky, and P. A. Crowell, Phys. Rev. Lett. **89**, 277201 (2002).
[3] B. B. Maranville, R. D. McMichael, S. A. Kim, W. L. Johnson, C. A. Ross, and J. Y. Cheng, J. Appl. Phys. **99**, 08C703 (2006).
[4] B. B. Maranville, R. D. McMichael, and D. W. Abraham, Appl. Phys. Lett. **90**, 232504 (2007).
[5] R. D. McMichael and B. B. Maranville, Phys. Rev. B **74**, 024424 (2006).
[6] J. Y. Cheng, C. A. Ross, E. L. Thomas, H. I. Smith, and G. J. Vansco, Appl. Phys. Lett. **81**, 3657 (2002).
[7] M. J. Donahue and D. G. Porter, in *Interagency Report NISTIR 6376* (National Institute of Standards and Technology, Gaithersburg, MD, 1999).
[8] R. D. McMichael and M. D. Stiles, J. Appl. Phys **97**, 10J901 (2005).
[9] C. Bayer, S. O. Demokritov, B. Hillebrands, and A. N. Slavin, Appl. Phys. Lett. **82**, 607 (2003).
[10] M. Bailleul, D. Olligs, and C. Fermon, Phys. Rev. Lett. **91**, 137204 (2003).
[11] B. B. Maranville, R. D. McMichael, C. L. Dennis, C. A. Ross, and J. Y. Cheng, IEEE Trans. Mag. **42**, 2951 (2006).
[12] C. Bayer, J. P. Park, H. Wang, M. Yan, C. E. Campbell, and P. A. Crowell, Phys. Rev. B **69**, 134401 (2004).